Lasers in Manufacturing Conference 2023

Mechanical properties of laser welded joints of wrought and heat-treated PBF-LB/M Inconel 718 parts depending on build direction

Juan Simón-Muzás[a,*], Christian Brunner-Schwer[b], Kai Hilgenberg[a], Michael Rethmeier[c,a,b]

[a]*Bundesanstalt für Materialforschung und -prüfung (BAM), 12205 Berlin, Germany*
[b]*Fraunhofer Institute for Production Systems and Design Technology, 10587 Berlin, Germany*
[c]*Institute of Machine Tools and Factory Management, Technische Universität Berlin, 10587 Berlin, Germany*

Abstract

Laser-based Powder Bed Fusion of Metal (PBF-LB/M) is a broadly used metal additive manufacturing (AM) method for fabricating complex metallic parts, whose sizes are however limited by the build envelope of PBF-LB/M machines. Laser welding arises as a valid joining method for effectively integrating these AM parts into larger assemblies.
PBF-LB/M components must usually be stress-relieved before they can be separated from the build plate. An additional heat treatment can be beneficial for obtaining homogeneous mechanical properties across the seam or for the formation of desired precipitations in nickel-based-alloys.
Therefore, the tensile performance of laser welded hybrid (AM/wrought) and AM-AM tensile samples of Inconel 718 is examined after undergoing three different heat treatments and considering three relevant build directions. It can be shown that the build orientation is an influencing factor on weld properties even after two applied heat treatments.

Keywords: Laser welding; PBF/LB-M; Hybrid components; Heat treatments; Build direction; Tensile performance; Inconel 718

1. Introduction

Inconel 718 is a precipitation strengthening nickel-basis superalloy with superior mechanical properties and performance [1]. Its intensive properties such as high hardness values and low thermal conductivity makes the alloy difficult to be processed employing conventional subtractive manufacturing methods, since these properties accelerate tool wear and consequently make such operations time-consuming and expensive [2] or even unfeasible. Furthermore, Inconel 718 covers nearly half of the total quantity of superalloys used in the world [3]. Therefore, this superalloy is especially attractive for the industry to be manufactured using PBF-LB/M, besides the advantages of this AM technology that eases the manufacturing of geometrically complex

parts with engineered inner cavities [4]. Nevertheless, size of PBF-LB/M components are limited by the build envelope of the machines. Moreover, using PBF-LB/M technology is usually not economically nor technically justified for simple components. The need of joining PBF-LB/M parts to other AM parts or to other simple i.e. wrought parts is a usual scenario in the process of integrating PBF-LB/M components into larger assemblies. Therefore, finding a joining technology without diminishing the mechanical properties of the part and of the joint is essential. Laser beam welding (LBW) arises as a valid option due to its versatility, narrow seam profile, small heat affected zone (HAZ) and relative limited distortion [5], some authors point out the superior tensile strength values of weldments with AM parts performed with LBW than with Electron Beam Welding (EBW) [6]. The mechanical behavior of joints in confluence with PBF-LB/M parts and in relation with PBF-LB/M factors, such as the build direction relative to the seam or the thermal condition, is fundamental. Few works are however devoted to determine and to quantify for a given metallic alloy, if the orientation of the layers of PBF-LB/M parts relative to the seam and to the tensile load play a relevant effect on the tensile performance of the joint when these parts are welded together or to a wrought conventional component of the same material. On the one hand, Zhang et al. 2021 [7] found that as-build 316L PBF-LB/M welded parts, whose layers are perpendicular to the seam, showed higher proof stress than those weldments whose layers are parallel to the seam due to the epitaxial grain growth relative to the loading direction. On the other hand, PBF-LB/M parts need to be stress-relieved with a heat treatment prior separation of the manufactured parts from the build plate. However, some authors point out that Inconel 718 in stress-relieved condition, according to standard, is not suitable for welding as liquation cracking is exacerbated and a second heat treatment is beneficial [8]. Thus, recrystallization and grain growth partially mitigate the anisotropic AM microstructure. Hence this assumed influence of the build orientation on the tensile performance of the joint could be reduced. In this respect, some works show that base-material PBF-LB/M Inconel 718 parts in as-build condition present lower strength than wrought parts of the same material as a result of the combined effect of interdendritic Laves precipitates and the free γ’ and γ’’ phases that lead to the generation of finer dislocate structures and then developed into a transgranular ductile fracture. Base-material in solution annealed condition exhibited higher mechanical strengths but lower ductility because of the presence of needle-like δ phases in the austenitic matrix and mainly in the grain boundaries but also within grains [9].

2. Experimental procedure

2.1. Wrought and PBF-LB/M sheets procuring and preparation

For testing the tensile performance of laser welded Inconel 718 PBF-LB/M parts together and to wrought parts of the same superalloy, series of flat tensile samples were manufactured and tested.
For this purpose, wrought hot-rolled sheets with dimensions 90.0 mm x 70.0 mm x 2.1 mm were procured. The exact chemical composition of the parts provided by the manufacturer ATI Metals is shown in Table 1. These sheets were obtained from a two-step hot-rolled plate (AMS 5596M) [10]. PBF-LB/M sheets of the same length and width but 2.7 mm thick were manufactured employing a SLM 280 HL machine of SLM Solutions Group AG, which operates with a 1070 nm continuous wave (cw) fiber laser with a maximum output of 400 W. Specimens were fabricated on a stainless steel AISI 314 build platform (280 mm x 280 mm x 25 mm) with a 4.0 mm high full-material volume support. The build platform was pre-heated at 200°C. The chamber was filled with Argon 5.0 and the oxygen concentration in the build chamber was kept under 0.15 vol% during the manufacturing process. To analyze the influence of the build direction relative to the seam, sheets were manufactured in three relevant build directions, namely 0°, 45° and 90° (Figure 1). Inconel 718 pre-alloyed gas-atomized powder provided by VDM Metals GmbH was used to manufacture the PBF-LB/M parts. Powder particles are spherical with an average particle size of 36 µm (15 µm - 53 µm) presenting a low level of satellites

and smooth surface, which is favourable for a good fluidity. The chemical composition from the specification sheet of the received batch is given in Table 1.

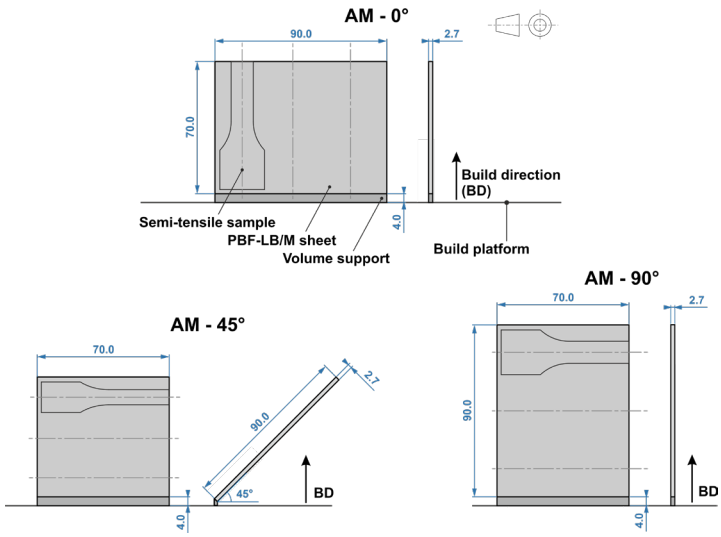

Fig. 1. Orientation of the PBF-LB/M sheets, corresponding to the three build directions considered and identified as AM-0°, AM-45°, and AM-90°. Support structures are colored in dark grey, which were removed before welding. Symmetry axes of the three semi-tensile specimens per sheet are represented together with the silhouette of one of these samples.

Table 1. Chemical composition of wrought sheets and PBF-LB/M Inconel 718 power batch used.

Element, wt%	Wrought	Powder
C	0.04	0.03
Mn	0.05	0.03
P	0.007	0.005
S	<0.001	0.001
Si	0.06	0.08
Cr	18.26	18.5
Ni	Bal.	Bal.
Al	0.49	0.5
Mo	2.91	3.1
Cu	0.02	0.02
Nb	5.11	5.19
Ta	0.01	0.01
Ti	1.05	0.89
Co	0.14	0.1
B	0.006	0.004
Fe	19.73	17.94

Before separating the samples, they were stress relieved (SR) at T = (1065 ± 15) °C for τ = 90 (-5, +15) min according to standard ASTM F3301 – 18a with the aim of reducing residual stresses generated in the building up process. Later, after separating them from the build plate, two groups of lattices were submitted to a second heat treatment: one to solution annealing (SA), and a second one to a standardized two-step aging (TSA). Targeted heat treatment cycles are shown in Table 2.

Table 2. Targeted heat treatments for PBF-LB/M sheets.

Condition	**Designation**	**Standard**	**Heat treatment schedules**			
			Heat treatment 1 – HT1 (Temperature, °C/ time, min)	**Cooling after HT1**	**Heat treatment 2 – HT2** (Temperature, °C/ time, min)	**Cooling after HT2**
Stress relieved	SR	ASTM F3301-18a	1065 / 90	Gas cooling, Ar	-	-
Solution annealed	SA	Adapt. AMS 5662	927 / 60	Gas quenching, N_2	-	-
Two-step aged	TSA	Adapt. AMS 5662	718 / 480	Vacuum	620 / 480	Gas cooling, Ar

2.2. Laser welding of sheets

Ready-to-weld sheets were joined with a Yb:YAG cw laser beam with a maximum output of 16 kW, a wavelength of 1030 nm and a beam parameter product of 8 mm x mrad by TRUMPF GmbH + Co. KG. The laser head is mounted on a 5-axis-gantry system. The laser beam is transmitted through a 200 µm optical fiber to the optics, with a focal length of 300 mm. The sheets were fixed with a clamping system that uniformly braced them along a surface on the opposite side and parallel to the welding edge. All welded pair of sheets were welded in butt position without employing any filler material and joined along the longest edge, which is 90.0 mm long. Argon 5.0 was used as shielding gas during the welding operation. The flow on the root side was provided through a stripping nozzle. A closed chamber that covers all the welding area was designed for the upper side, which receives the laser beam. The chamber was fixed on the clamps and included a slot along the welding track but covered with a lid provided with a hole. This lid slid on the upper chamber surface in unison with the laser beam, as it is fixed with the laser head. Moreover, it was long enough so that it covered the whole slot length in any point of the weld track. A sketch of the whole assembly is shown in Figure 2. The laser welding parameters used for welding all pair of sheets consisted of a welding power of P = 1400 W, a welding speed of v_S = 1000 mm/min with a focus shift of f = +5 mm.

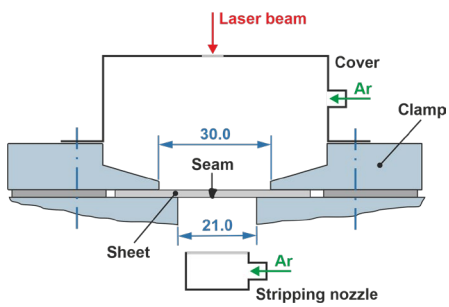

Fig. 2. Drawing showing the fixation of two sheets between the clamps and the position of the argon nozzles.

2.3. Manufacturing of tensile samples out of the welded sheets

From each pair of welded sheets, three flat tensile samples (type E) were obtained according to the standard DIN EN ISO 4136 [11]. The weld is placed in the middle of the reduced section of the tensile sample (Figure 3). The exact profile was obtained by wire eroding, whose theoretical surface quality of the cut remains under the roughness value pointed by the standard. The slight difference in thickness of the procured and manufactured plates resulted not relevant to the welding process and seam geometry, and it served to remove any eventual imperfections such as groove, excess of penetration on the root or excess of weld metal on the head, as the standard clearly appoints its removal from the tensile sample. In addition, as-build PBF-LB/M samples presented different roughness on its respective surfaces (i.e. up-skin, down-skin) that lie above the mentioned limit marked by the standard. For this reason the thickness of the PBF-LB/M sheets was slightly bigger than the wrought. Thus, the upper and lower surfaces of samples were milled, so that the sample thickness at any point was 2.0 (0, +0.2) mm.

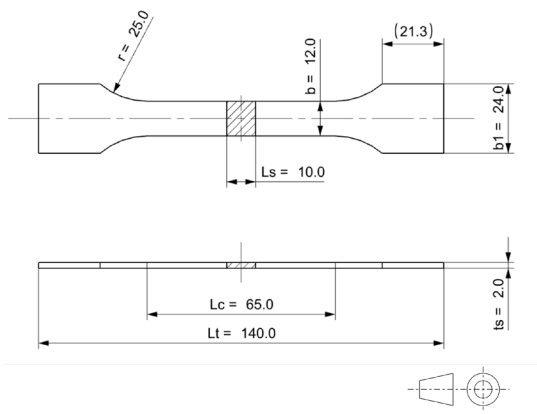

Fig. 3. Drawing corresponding to a flat tensile sample according to standard DIN EN ISO 4136 [12]

2.4. Laser welding of sheets

For each combination, six tensile samples were tested obtained from two pairs of sheets welded together. Quasi-static tensile tests were undertaken using an electromechanical controlled universal tensile machine *Model 4505* manufactured by *Instron* to evaluate the strength of the laser welded joints in line with DIN EN ISO 6892-1 [13]. The dimensions of the coupons were measured using a digital micrometer. For measuring the dimensions of the cross-section at the breaking point, a digital caliper was used. A class 0.5 clip-on extensometer Type *634.25F-25* produced by *MTS Systems* and with a recording frequency of 20 Hz was used to determine the deformation when the load is applied. The 0.2 % offset yield strength was derived from the load-displacement curve. For tensile samples whose condition provides small tensile toughness, a single estimated strain rate over the parallel length of $\dot{e}_{Lc}$= 0.0025 s^{-1} was used. For samples with a condition leads to bigger toughness values, two strain rates were employed in conjunction with the standard: a first strain rate of $\dot{e}_{Lc}$= 0.0025 s^{-1} until a strain value of 1.0 %, and a second strain until rupture of $\dot{e}_{Lc}$= 0.0067 s^{-1}. A coupon of a central part of the seam was procured and embedded in graphite-based resin and etched with Kalling's No. 2 reagent. Bright-field images of the cross section were taken with a light microscope to detect potential weld imperfections. The surface fracture was analyzed both with light microscope and the areas of interest with SEM.

3. Results

3.1. Tensile properties

In Figures 4a and 4b, AMS nominal specification values of yield strength ($R_{p0.2\%}$), ultimate tensile strength (R_m) and elongation at break (A) for cast (AMS 5662 [14]) and wrought (AMS 5996M [10]) base materials are shown. On the one hand, tested AM-wrought and AM-AM welded specimens in SR+SA condition presented the fracture on the base material additive manufactured side mostly, far from the HAZ. On the other hand, samples in SR+TSA condition exhibited the cleavage in the weld and only five of them failed on the wrought side base material. The influence of the build direction (0°, 45° and 90°) and the heat-treated condition (SR+SA and SR+TSA) of the PBF-LB/M sheets on the tensile performance is shown in Figure 5. Overall, ultimate yield strength vales of welded specimens are comparable to cast material and are much lower than the wrought base material, as Zhang et al., 2015 [9] similarly concludes after testing entirely PBF-LB/M manufactured tensile samples of Inconel 718. In contrast, average yield strength values of welded samples in SR+SA condition are almost 50 % smaller than that of cast material (Figures 5a and 5b). This difference is however reduced to about 10 % for the combination AM-AM in SR+TSA condition (Figure 5d). Regarding the elongation at break (Figure 6), joined specimens in SR+SA condition show much more higher values for all build directions than those in SR+TSA condition, especially for the combination AM-AM in SR+TSA condition (Figure 6d).

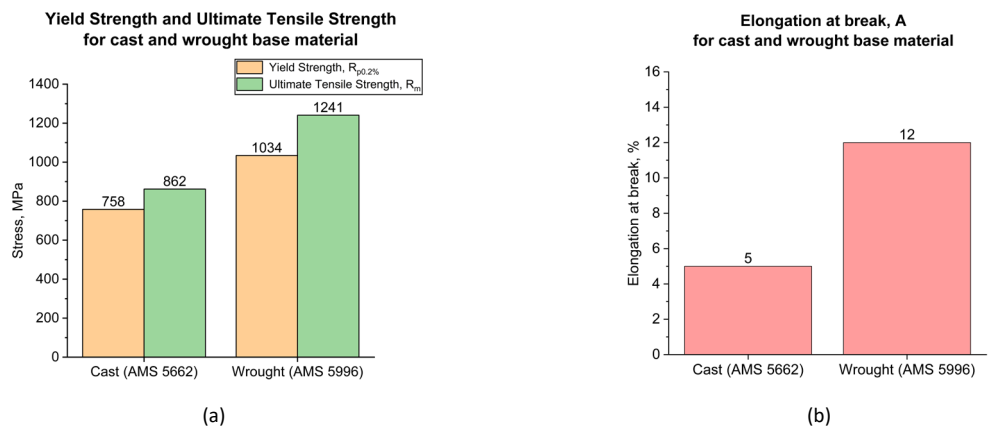

Fig. 4. Nominal mechanical tensile properties of cast (AMS 5662 [14]) and wrought (AMS 5996M [10]) Inconel 718 base material.

Yield strength values remain constant across all AM build directions and for both combinations (AM-wrought and AM-AM) whose AM parts are in SR+SA condition (Figures 5a and 5b). The combinations AM-wrought in SR+SA condition for 0° and 90° build direction have similar ultimate tensile strength values. In contrast, the combination with AM 45° build direction has in average 15 % less tensile strength. An inferential statistical test ANOVA with an interval of confidence of 95 % has confirmed the statistical significance of the results. The arithmetic mean of elongation at break (A) and necking (Z) for this orientation is also about 35 % smaller than those for the other two build directions (Figure 6a).

R_m values for the combination AM-AM in SR+SA condition are similar but the large standard deviation for the 0° build direction (Figure 6b) is explained through the presence of a PBF-LB/M imperfect layer due to lack-of-fusion that affected the three tensile samples obtained from the same welded sheet. Arithmetic means of the three tensile samples obtained from every pair of welded sheets are shown separately in Figure 7a and 7b. Samples obtained from the combination with this AM imperfection (*welded pair I*) show a 35 % less tensile

strength than the flawless *welded pair II*. Conversely, the yield strength and as well the elastic region is not affected by the presence of these imperfections.
It can be also observed that within the combination AM-wrought in SR+TSA condition the 45° build direction appears to be the weakest (Figure 5c). Nevertheless, the elongation at break mean of the AM 0°-wrought category shows a surprisingly larger standard deviation (Figure 6c). Analogously, the low values observed in the hybrid combinations (AM-wrought) with a 45° AM part are not translated to the AM-AM combinations, but AM-AM 90° presents a much smaller ultimate tensile strength. This result is contrary to the one presented by Zhang et al., 2021 [7] with 316L, as in their research samples whose layers are oriented perpendicular to the seam, the proof stress is higher. After representing the values of the three tensile samples from each pair of welded sheets, namely *welded pair I* and *II* (Figure 7c and 7d), the difference in values among the two group of samples is remarkable. Samples from the called *welded pair I* presented lack-of-fusion imperfection in one of the layers as well. All tensile samples from the *welded pair II* failed at a midpoint of the wrought side, whereas tensile samples from *welded pair I* failed on the AM-side right next to the seam and along the identified defective layer (Figures 8a and 8b). Finally, it is also remarkable the low ultimate tensile strength value of the AM 90° build direction for the AM-AM combination in SR+TSA condition in comparison with the other two build directions (Figure 5d).
Overall, it can be observed that elongation at break and necking average values present a much larger standard deviation than the strength values. Furthermore, the described tendencies through the arithmetic means are more pronounced in elongation and necking charts than in stress bar charts.

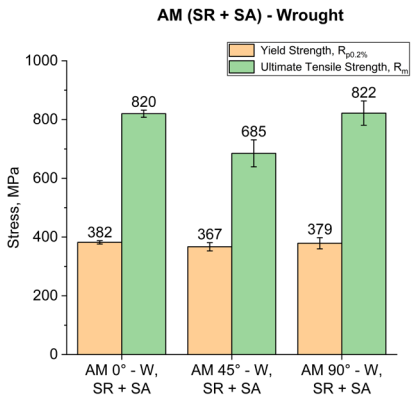

(a)

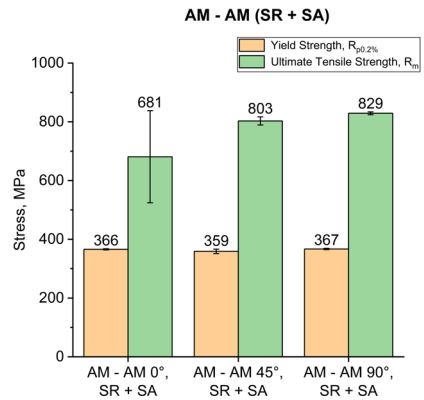

(b)

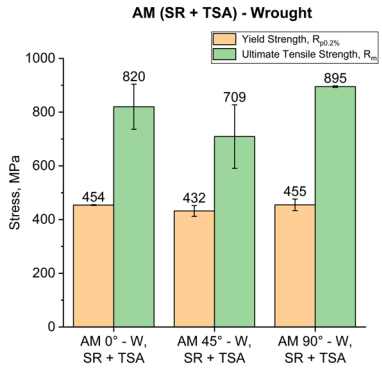

(c)

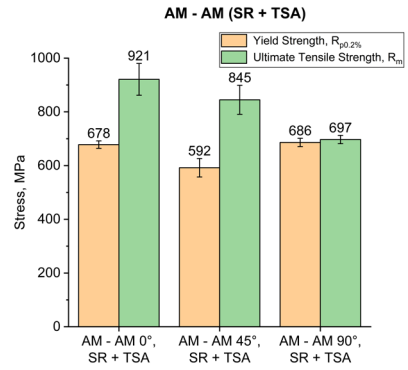

(d)

Fig. 5. Yield strength ($R_{p0.2\%}$) and ultimate tensile strength (R_m) average values of AM-wrought and AM-AM combinations for the three build directions (0°, 45° and 90°) and two heat treatment conditions (SR + SA and SR + TSA) of the PBF-LB/M parts.

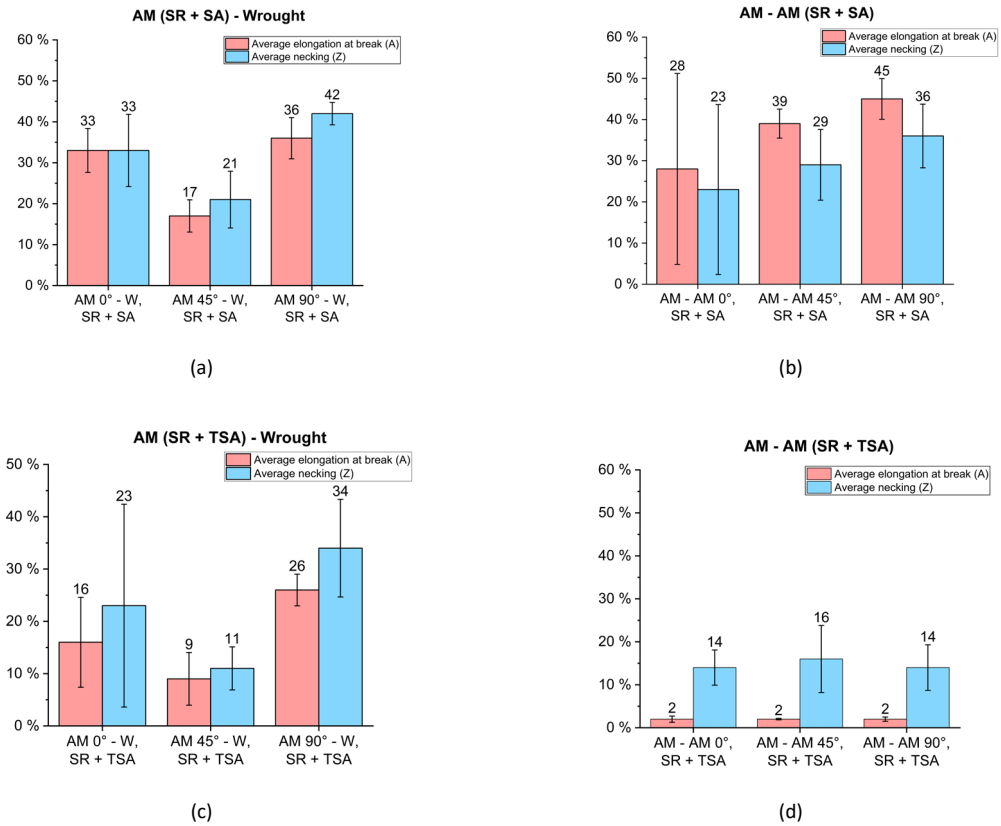

Fig. 6. Elongation at break (A) and necking (Z) average values of AM-wrought and AM-AM combinations for the three build directions (0°, 45° and 90°) and two heat treatment conditions (SR + SA and SR + TSA) of the PBF-LB/M parts.

Fracture surface of the tested specimens present a dimpled surface, indicating a transgranular ductile failure mode. Some of the tensile samples present a 45° to the tensile axis fracture, the direction in which the shear stress is maximum. It has been observed that ductility is strongly dependent on the condition of the PBF-LB/M part. Tensile specimens with AM in SR+SA condition present the largest ductility values, exhibited through large elongation at break values, some of them slightly lower than 50 %. It is expected, as this condition provides a microstructure that favors ductility. On the other hand, samples whose AM part was in SR+TSA condition show the largest tensile toughness but at expenses of ductility. In particular AM-AM in this condition present the highest tensile strength values, some higher than 900 MPa. It is also noteworthy, that $R_{p0.2\%}$ values for the AM-AM SR+TSA category are 30 % higher than for the AM-wrought category in the same condition.

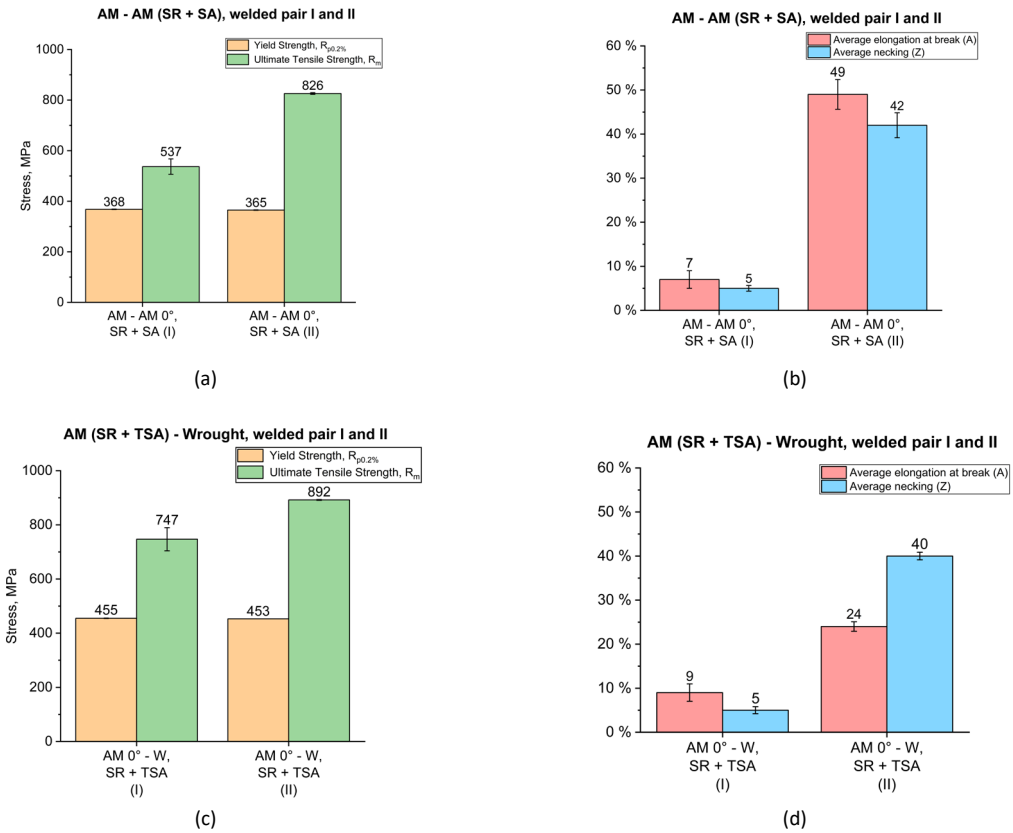

Fig. 7. Separate representation of the mechanical properties analyzed grouped in the two pairs of welded sheets for the combination AM-AM 0° in SR+SA condition and AM 0°-wrought in SR+TSA condition, since the combined arithmetic mean presented a to large standard deviation as a result of Lack-of-Fusion in the PBF-LB/M sheet of one of the welded pair (in the charts accounted as welded pair I)

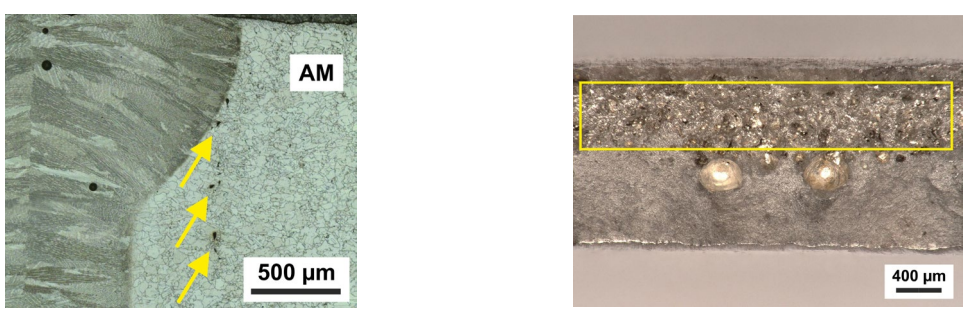

Fig. 8 (a) Coupon of the two welded specimens corresponding to *welded pair I* AM-AM 0° in SR+TSA condition. The yellow arrows point out the defective AM layer with a Lack-of-Fusion porosity. (b) View of the fracture surface of one of the tensile samples located at the same plane where this imperfection (marked within the yellow rectangle) was identified.

4. Conclusions

Laser Beam Welding shows to be a suitable process for welding PBF-LB/M parts of Inconel 718 together and to wrought parts of the same material. The welded joints present ultimate tensile strength vales similar to the cast base material but less than the wrought base. The combination AM-wrought for both studied conditions SR+SA and SR+TSA, whose PBF-LB/M part oriented in 45° build direction, presents the lowest average values of ultimate tensile strength and elongation. In contrast, yield strength values and its elastic region appears to be not influenced by the AM build direction and present similar values across the three orientations considered. This finding is not extrapolative to AM-AM combinations that do not depict a clear fall of properties for the 45° build direction. In addition, a statistical inferential test ANOVA has confirmed the relevance of this observation for the AM-wrought combination in SR+SA condition, but not for the SR+TSA condition. Fracture surfaces in the AM, wrought or the seam are dimpled, characteristic for a transgranular ductile failure mode, besides the fracture caused by PBF-LB/M characteristic lack-of-fusion defects, which clearly detriments the mechanical properties of the joints. However, yield strength and the elastic region appears not to be affected. The presence of this porosity, which is spread across one of the layers for the 0° build direction, serves as a perfect plane for the propagation of the fracture. Strength values of PBF-LB/M Inconel 718 sheets welded together and to wrought ones of the same material are comparable to those of cast Inconel 718. The reason behind is probably the partial recrystallization and grain growth of PBF-LB/M parts as a result of the heat treatments.

Acknowledgements

The authors are grateful for the financial support from the *Deutsche Forschungsgemeinschaft* (DFG, German Research Foundation), project number 429808811.

References

[1] Popovich, V.A., Borisov, E.V., Popovich, A.A., Sufiiarov, V.Sh., Masaylo, D.V., Alzina, L., 2017. Impact of heat treatment on mechanical behaviour of Inconel 718 processed with tailored microstructure by selective laser melting, Materials & Design 131, pp. 12-22.
[2] Wang, X., Gong, X., Chou, K., 2017. Review of powder-based laser additive manufacturing of Inconel 718 parts, Journal of Engineering Manufacture 231, pp. 1890-1903.
[3] Rautio, T., Mäkikangas, J., Kumpula, J., Järvenpää, A., Hamada, A., 2021. Laser welding of laser powder bed fusion manufactured Inconel 718: Microstructure and mechanical properties, Key Engineering Materials 883, p. 234.
[4] Casalino, G., Campanelli, S.L., Ludovico, A.D., 2013. Laser-arc hybrid welding of wrought to selective laser molten stainless steel, International Journal of Additive Manufacturing Technology 68, pp. 209-216.
[5] Hu, X., Xue, Z., Zhao, G., Yun, J., Shi, D., Yang, X., 2019. Laser welding of a selective laser melted Ni-base superalloy: Microstructure and high temperature mechanical property, Materials Science & Engineering A 745, p. 336.
[6] Tavlovich, B., Shirizly, A., Katz, R., 2018. EBW and LBW of Additive Manufactured Ti6Al4V Products, Welding Journal 97, p. 189
[7] Zhang, R, Buchanan, C., Matilainen, V.-P., Daskalaki, D., Ben Britton, T., Piili, H., Salminen, A., Gardner, L., 2021. Mechanical properties and microstructure of additively manufactured stainless steel with laser joints, Materials & Design 208
[8] Muralidharan, B.G., Shankar V., Gill, T.P.S., 1996. Weldability of Inocnel 718 – A Review, Indira Gandhi Centre for Atomic Research Kalpakkam. Department of Atomic Energy, Government of India.
[9] Zhang, D., Niu, W., Cao, X., Liu, Z., 2015. Effect of standard heat treatment on the microstructure and mechanical properties of selective laser melting manufactured Inconel 718 superalloy, Materials Science & Engineering A 644, p. 39.
[10] S.A.E. Aerospace, Aerospace Material Specification: AMS 5996M, SAE International, 2012.
[11] ASTM F3301-18a, Standard for Additive Manufacturing – Post Processing Methods - Standard Specification for Thermal Post-Processing Metal Parts Made Via Powder Bed Fusion, ASTM International, 2018.
[12] DIN EN ISO 4136, Destructive tests on welds in metallic materials – Transverse tensile test, DIN Deutsches Institut für Normung, 2013.
[13] DIN EN ISO 6892-1, Tensile testing – Part 1: Method of test at room temperature, DIN Deutsches Institut für Normung, 2017.
[14] S.A.E. Aerospace, Aerospace Material Specification: AMS 5662, SAE International, 2012.